Atmos. Chem. Phys. Discuss., 14, 23745–23761, 2014
www.atmos-chem-phys-discuss.net/14/23745/2014/
doi:10.5194/acpd-14-23745-2014

Atmospheric Chemistry and Physics Discussions

The role of convective overshooting clouds in tropical stratosphere–troposphere dynamical coupling

K. Kodera[1,2], B. M. Funatsu[3,4], C. Claud[4], and N. Eguchi[5]

[1]Solar-Terrestrial Environment Laboratory, Nagoya University, Nagoya, Japan
[2]Climate and Ecosystems Dynamics Division, Mie University, Tsu, Japan
[3]LETG-Rennes COSTEL, Université Rennes 2, Rennes, France
[4]Laboratoire de Météorologie Dynamique, Ecole Polytechnique, Palaiseau, France
[5]Research Institute for Applied Mechanics, Kyushu University, Kasuga, Japan

Received: 26 August 2014 – Accepted: 3 September 2014 – Published: 15 September 2014

Correspondence to: K. Kodera (kodera@stelab.nagoya-u.ac.jp)

Published by Copernicus Publications on behalf of the European Geosciences Union.

Abstract

This paper investigates the role of deep convection and overshooting convective clouds in stratosphere–troposphere dynamical coupling in the tropics during two large major stratospheric sudden warming events in January 2009 and January 2010. During both events, convective activity and precipitation increased in the equatorial Southern Hemisphere as a result of a strengthening of the Brewer–Dobson circulation induced by enhanced stratospheric planetary wave activity. Correlation coefficients between variables related to the convective activity and the vertical velocity were calculated to identify the processes connecting stratospheric variability to the troposphere. Convective overshooting clouds showed a direct relationship to lower stratospheric upwelling at around 70–50 hPa. As the tropospheric circulation change lags behind that of the stratosphere, outgoing longwave radiation shows almost no simultaneous correlation with the stratospheric upwelling. This result suggests that the stratospheric circulation change first penetrates into the troposphere through the modulation of deep convective activity.

1 Introduction

Weather forecasting in tropical regions is challenging due to the unstable nature of the atmosphere there and its sensitivity to various extratropical disturbances. The impact of the extratropical circulation on the tropics, such as the lateral propagation of tropospheric Rossby waves, has been studied previously (e.g., Kiladis and Weickmann, 1992; Funatsu and Waugh, 2008). The influence from above (i.e., from the stratosphere) is generally neglected, but under certain circumstances, such as during a sudden stratospheric warming (SSW) event, stratospheric meridional circulation change can modify convective activity as will be shown later.

Early satellite measurements showed that enhanced poleward eddy heat fluxes in the extratropical stratosphere induce tropical cooling through changes in the mean

meridional circulation (Fritz and Soules, 1970; Plumb and Eluszkiewicz, 1999; Randel et al., 2002). It is generally believed that such changes in the stratosphere do not affect the troposphere, due to the difference in air density between the two. Indeed, tropical temperature change induced by the intraseasonal mean meridional circulation is apparent only in the layer around 70 hPa and above (Ueyama et al., 2013).

However, this does not imply that the stratospheric meridional circulation has no impact on the atmosphere below the 70 hPa level. A possible impact of stratospheric meridional circulation on cumulus heating has been suggested by Thuburn and Craig (2000) in a simplified general circulation model experiment. Stratospheric upwelling effects on tropical convection is also confirmed by a more realistic general circulation model forecast study (Kodera et al., 2011a). These models make use of cumulus parameterization to account for the effect of convection into large scale circulation. Therefore, model sensitivity should be dependent on the parameterization used. Stratospheric effect on tropical convection is also found in non-hydrostatic models that treat the convection explicitly.

Although it is not fully understood yet how stability influences anvil cloud-top height, Chae and Sherwood (2010) showed with observational data and a regional non-hydrostatic model experiment that the variation of static stability near the tropopause due to a change in the stratospheric upwelling, influences cloud height even the cloud height peaks only near 12 km (or 200 hPa). Using a global non-hydrostatic model simulation, Eguchi et al. (2014) also found that increased tropical upwelling due to a SSW event reduces the static stability in the upper Tropical Tropopause layer (TTL), which leads to an increase of deep convective activity in the troposphere.

Temperature response to stratospheric upwelling becomes unclear in the region lower than the tropopause because clouds form in response to adiabatic cooling associated with upwelling. Stratospheric temperature decrease, but minimal temperature change in the TTL, results in a decrease in static stability in the upper TTL (Li and Thompson, 2013). In the regions where deep convective clouds are frequent, stratospheric influence further penetrates deeper in the troposphere (Eguchi and Kodera,

2010; Kodera et al., 2011b). Once the distribution of convective clouds is modified, this effect can be amplified within the troposphere through a feedback involving water vapour transport (Eguchi and Kodera, 2007).

Here, we focus on the role of overshooting and deep convective clouds in stratosphere–troposphere dynamical coupling in the tropics, and present case studies of two of the recent largest SSW events in January 2009 and January 2010 (Harada et al., 2010; Ayarzagüena et al., 2011). It should be noted, however, that not all major SSW events necessarily have large tropical impacts, as this depends on the latitude of the wave breaking (Taguchi, 2011).

2 Data

Meteorological reanalysis data from the European Centre for Medium–Range Forecasts (ECMWF) ERA interim (Dee et al., 2011) were used to analyze air temperature and winds. Cloud data in the TTL, the Level 2 Cloud Layer Product (Version3-01) were obtained by Cloud–Aerosol LIdar with Orthogonal Polarization (CALIOP) aboard CALIPSO satellite (Winker et al., 2007). Outgoing longwave radiation (OLR) data provided by NOAA (e.g., Arkin and Ardanuy, 1989) is widely used to analyse convective activity in the tropics. In this study, in addition to the OLR data with a $2.5^{\circ} \times 2.5^{\circ}$ lat/lon resolution, we used the Microwave Humidity Sensor (MHS) data, obtained from NOAA18 and MetOp-A, to capture deep convective activity. The equatorial crossing time for these platforms is approximately 14:00 local time (LT) for NOAA18, and 21:30 LT for MetOp-A. In the present work, the original data was regridded to a regular grid with resolution of 0.25 lat × 0.25 lon. The figures show DC and COV occurrences resampled to a grid of 2.25 × 2.25 for plotting purposes.

To capture deep, precipitating clouds we used the diagnostic developed for the tropics by Hong et al. (2005), which is based on the brightness temperature differences (ΔT) measured by three channels of the MHS between: (i) 183.3 ± 1 and 183.3 ± 7 GHz ($\Delta T17$), (ii) 183.3 ± 1 and 183.3 ± 3 GHz ($\Delta T13$); and (iii) 183.3 ± 3 and 183.3 ± 7 GHz

($\Delta T37$). Deep convective cloud (DC) and convective overshooting (COV) were discriminated according to the following criteria, in which COV refers to clouds able to penetrate into the tropopause region (Hong et al., 2005; Funatsu et al., 2012). Deep convective cloud: $\Delta T17 \geq 0$, $\Delta T13 \geq 0$, $\Delta T37 \geq 0$ K; and convective overshooting: $\Delta T17 \geq \Delta T13 \geq \Delta T37 > 0$ K.

The Tropical Rainfall Measuring Mission (TRMM) daily-integrated precipitation (TRMM 3B42 v7) was used to study surface precipitation (Huffman et al., 2007).

3 Results

Enhanced Brewer–Dobson (BD) circulation during a stratospheric warming event creates strong downwelling in the polar region and upwelling in the tropical stratosphere, and thus warming and cooling tendency in respective regions. Figure 1a and b shows the evolution of eddy heat flux at 100 hPa averaged over the extratropical NH (45° N–75° N), and the latitude–time section of the zonal mean pressure coordinate vertical velocity at 50 hPa from 1 January to 11 February (the left and right panels are for 2009 and 2010, respectively). In both years, stratospheric upwelling in the tropics at the 50 hPa level strengthens following the increase in wave activity at around 16 January in 2009, and around 20 January (indicated by the solid vertical lines in the figure). In the tropics, an increase in COV is synchronous with the stratospheric upwelling (Fig. 1c). The convective activity represented by the OLR also increases in the SH, which can also be characterized as a southward shift of the active convective region (Fig. 1d). A delay in the response of the OLR in the SH is also noted.

To study the relationship between tropospheric convective activity and the vertical velocity at different pressure levels, correlation coefficients were calculated between variables representing a convective activity (COV, DC, and OLR) and the pressure vertical velocity (ω) at each level (Fig. 2). Variables were first averaged over the tropics (25° S to 25° N) and then correlations were calculated for the 31 day period centred on the onset day (16 January for 2009 and 20 January for 2010). For convenience of

comparison, the sign of the OLR was reversed (–OLR). In both winters, COV shows the highest correlation with ω in the lower stratosphere around 70–50 hPa. DC is also correlated with the stratospheric upwelling, but less so. The OLR shows little relationship with the stratospheric circulation, although it is correlated with vertical velocity in the troposphere.

It is reasonable to expect that stratospheric vertical velocity should have the strongest relationship with the occurrence of COV (i.e., convection penetrating to the stratosphere) and the weakest relationship with OLR, which is sensitive to lower clouds as well as deep convection. Therefore, the following inequalities among the correlation coefficient, r, between the lower stratospheric pressure vertical velocity, ω, should be expected:

$$r_{\omega,\mathrm{COV}} < 0, \quad |r_{\omega,\mathrm{COV}}| > |r_{\omega,\mathrm{DC}}|, \quad |r_{\omega,\mathrm{DC}}| > |r_{\omega,-\mathrm{OLR}}|, \tag{1}$$

where $r_{\omega,\mathrm{COV}}$, $r_{\omega,\mathrm{DC}}$, and $r_{\omega,-\mathrm{OLR}}$ are the correlation coefficients between ω and COV, DC, or –OLR, respectively.

If there is no physical relationship among the variables, such conditions are satisfied in $(1/2)^3$ of the cases by chance. In the present case, this occurred during two winters, so that the probability that this happened by chance is $(1/2)^6$; i.e., only about 1.5 % of the cases. If the COV, DC, and OLR were strongly correlated to each other, correlation coefficients would be similar, which makes the Eq. (1) less satisfied. This result supports our working hypothesis that lower stratospheric vertical velocity variation is coupled with the tropical convective activity.

Figure 3 depicts a development of downward coupling in the equatorial summer tropics, averaged between 20° S and the equator. The temperature tendency (Fig. 3a) shows a rapid decrease in the stratosphere following the increase in the eddy heat flux in Fig. 1a, but no clear temperature signal is observed in the troposphere, which agrees with the results of previous study (Ueyama et al., 2013). Figure 3b shows altitude–time section of measured cloud frequency (optical thickness < 4) by CALIOP. Horizontal dashed lines indicate approximate height corresponding to 100 hPa pressure level

(solid lines in Fig. 3a and c). Prior to the SSWs, thin clouds are formed near16.6 km (or 100 hPa) around a cold point tropopause. When cooling events start, cloud forms all the depth of the TTL, indicating a development of convective activity. Pressure vertical velocity is shown as departure from the period mean normalized by a daily standard deviation at each level to visualize the large range of variation (Fig. 3c). Although vertical velocity varies in a similar manner to temperature tendency in the stratosphere, an increase in the upwelling also occurs in the troposphere following the stratospheric change. This tropospheric upwelling is associated with an increase in surface precipitation (Fig. 3d).

This result shows that the temperature tendency is a good proxy for vertical velocity in the stratosphere. However, dynamical cooling tends to be compensated by diabatic heating due to cloud formation lower than the tropopause as illustrated in Fig. 3; consequently, the temperature tendency is no longer a good indicator of the vertical velocity below 70 hPa.

Figure 4 shows the evolution of the geographical distribution of OLR and COV before (i), and after (ii) the onset of the event. The influence of the El Niño Southern Oscillation (ENSO) is evident in the OLR during period (i). In January 2009, which is a cold phase of ENSO, a well-developed region of low OLR is located over the Maritime Continent, while in January 2010, a warm phase of ENSO, it is located over the western Pacific according to the change in the equatorial Pacific sea surface temperature (SST). The velocity potential at 925 hPa (contour lines in Fig. 4a) indicates that these convective activities are maintained by a large-scale low-level convergence. After the onset of the stratospheric event during period (ii), the low-OLR centre over the Maritime Continent or western Pacific is weakened, and multiple convective-active regions develop in the SH along 15° S. This active convective zone includes tropical cyclones and storms (names are indicated below the panel) over warm ocean sectors near Madagascar, North of Australia, and in the southwestern Pacific.

The occurrence of COV (Fig. 4b) is high over the African and South American continents, but no particular enhancement is seen around the Maritime Continent–western

Pacific region. This indicates the weaker dependency of COV on low-level convergence. Although the occurrence of COV increases after the onset in period (ii), no substantial change is seen in the spatial structure except that the COV distribution takes a more zonal form. The distribution of the regions with low OLR becomes increasingly similar to that of COV during period (ii). This indicates that the COV-related deep convective activity becomes important after the onset of the stratospheric event.

4 Summary and discussion

The results of our analysis of changes in tropical circulation associated with large SSWs during January 2009 and January 2010 can be summarized as follows.

Enhanced stratospheric wave activity produced a cooling in the tropical stratosphere through a strengthening of the BD circulation. This influence penetrated downward into the troposphere through a change in the cloud formation. Among the variables representing different convective activity, COV shows the highest correlation with the lower stratospheric vertical velocity. This result is reasonable because the COV clouds can penetrate above the tropopause and interact directly with the stratospheric circulation. The reason of low correlation of the OLR with stratospheric upwelling originates from the fact that the tropospheric variation lags by about a week (Fig. 1).

The results obtained from our two case studies are consistent with earlier results from an independent composite analysis of the winters between 1979 and 2001 (Kodera, 2006), which revealed that the tropospheric convective activity in the equatorial SH is enhanced following the stratospheric equatorial upwelling induced by upward propagation of planetary waves during the NH winter.

As for a process which relates tropical stratospheric upwelling and the tropospheric convective activity, investigation between the diabatic heating in the TTL and the stratospheric vertical velocity is crucial. Direct measurement of such quantities are difficult, but a global non-hydrostatic model study (Eguchi et al., 2014) confirmed the relationship suggested in the present result.

The characteristics of the convective activity changed following the stratospheric event. When stratospheric upwelling was suppressed before onset of the event, convection tended to cluster around the equatorial Maritime Continent or western Pacific region depending on the phase of ENSO. When the stratospheric upwelling increased, convection expanded over a wide range of longitudes in the tropical summer hemisphere. In other words, tropical circulation changed from a more Walker like (east–west) configuration to a more Hadley (north–south) type.

The Madden–Julian Oscillation (MJO) (Madden and Julian, 1994) has a significant influence on tropical convective activity. One would ask whether or not the present phenomenon is associated with the MJO. The features of the MJO in January 2009 and 2010 differed significantly as can be seen in Fig. 5. A convective centre remained stationary over the Maritime Continent prior to the onset of the 2009 stratospheric event, after which an eastward propagation was initiated from the Indian Ocean. In contrast, an eastward propagating convective centre became almost stationary over the western Pacific after the onset in January 2010. In spite of the differences in the MJO in January 2009 and 2010, circulation changes related to the stratospheric events showed similar features during both winters, suggesting that the present phenomenon is independent of the MJO.

Acknowledgements. We thank R. Ueyama, T. Nasuno and C. Kodama for useful comments and discussion. This work was supported in part by JSPS Grants-in-Aid for Scientific Research (S)24224011 and (C)25340010. B. M. Funatsu and C. Claud acknowledge the support of DGA and CNES. MHS data were obtained through the French Mixed Service Unit ICARE. CALIOP data were from ASDC (Atmospheric Science Data Center) at NASA. TRMM data were acquired through the Giovanni online data system, developed and maintained by NASA GES DISC.

References

Arkin, P. A. and Ardanuy, P. E.: Estimating climate-scale precipitation from space: a review, J. Climate, 2, 1229–1238, 1989.

Ayarzagüena, B., Langematz, U., and Serrano, E.: Tropospheric forcing of the stratosphere: a comparative study of the two different major stratospheric warmings in 2009 and 2010, J. Geophys. Res., 116, D18114, doi:10.1029/2010JD015023, 2011.

Chae, J.-H. and Sherwood, S. C.: Insights into cloud-top height and dynamics from the seasonal cycle of cloud-top heights observed by MISR in the West Pacific region, J. Atmos. Sci., 67, 248–261, 2010.

Dee, D. P., Uppala, S. M., Simmons, A. J., Berrisford, P., Poli, P., Kobayashi, S., Andrae, U., Balmaseda, M. A., Balsamo, G., Bauer, P., Bechtold, P., Beljaars, A. C. M., van de Berg, L., Bidlot, J., Bormann, N., Delsol, C., Dragani, R., Fuentes, M., Geer, A. J., Haimberger, L., Healy, S. B., Hersbach, H., Hólm, E. V., Isaksen, L., Kållberg, P., Köhler, M., Matricardi, M., McNally, A. P., Monge-Sanz, B. M., Morcrette, J.-J., Park, B.-K., Peubey, C., de Rosnay, P., Tavolato, C., Thépaut, J.-N., and Vitart, F.: The ERA-Interim reanalysis: configuration and performance of the data assimilation system, Quart. J. R. Meteorol. Soc., 137, 553–597, 2011.

Eguchi, N. and Kodera, K.: Impact of the 2002, Southern Hemisphere, stratospheric warming on the tropical cirrus clouds and convective activity, Geophys. Res. Lett., 34, L05819, doi:10.1029/2006GL028744, 2007.

Eguchi, N. and Kodera, K.: Impacts of stratospheric sudden warming on tropical clouds and moisture fields in the TTL: a case study, SOLA, 6, 137–140, 2010.

Eguchi, N., Kodera, K., and Nasuno, T.: A global non-hydrostatic model study of a downward coupling through the tropical tropopause layer during a stratospheric sudden warming, Atmos. Chem. Phys. Discuss., 14, 6803–6820, doi:10.5194/acpd-14-6803-2014, 2014.

Fritz, S. and Soules, S. D.: Large-scale temperature changes in the stratosphere observed from Nimbus III, J. Atmos. Sci., 27, 1091–1097, 1970.

Funatsu, B. M. and Waugh, D. W.: Connections between potential vorticity intrusions and convection in the eastern tropical Pacific, J. Atmos. Sci., 65, 987–1002, 2008.

Funatsu, B. M., Dubreuil, V., Claud, C., Arvor, D., and Gan, M. A.: Convective activity in Mato Grosso state (Brazil) from microwave satellite observations: comparisons between AMSU and TRMM data sets, J. Geophys. Res., 117, D16109, doi:10.1029/2011JD017259, 2012.

Harada, Y., Goto, A., Hasegawa, H., Fujikawa, N., Naoe, H., and Hirooka, T.: A major stratospheric sudden warming event in January 2009, J. Atmos. Sci., 67, 2052–2069, 2010.

Hong, G., Heygster, G., Miao, J., and Kunzi, K.: Detection of tropical deep convective clouds from AMSU-B water vapor channels measurements, J. Geophys. Res., 110, D05205, doi:10.1029/2004JD004949, 2005.

Huffman, G. J., Bolvin, D. T., Nelkin, E. J., Wolff, D. B., Adler, R. F., Gu, G., Hong, Y., Bowman, K. P., and Stocker, E. F.: The TRMM Multisatellite Precipitation Analysis (TMPA): quasi-global, multiyear, combined-sensor precipitation estimates at fine scales, J. Hydrometeorol., 8, 38–55, 2007.

Kiladis, G. N. and Weickmann, K. M.: Extratropical forcing of tropical Pacific convection during northern winter, Mon. Wea. Rev., 120, 1924–1939, 1992.

Kodera, K.: Influence of stratospheric sudden warming on the equatorial troposphere, Geophys. Res. Lett., 33, L06804, doi:10.1029/2005GL024510, 2006.

Kodera, K., Mukougawa, H., and Kuroda, Y.: A general circulation model study of the impact of a stratospheric sudden warming event on tropical convection, SOLA, 7, 197–200, 2011a.

Kodera, K., Eguchi, N., Lee, J.-N., Kuroda, Y., and Yukimoto, S.: Sudden changes in the tropical stratospheric and tropospheric circulation during January 2009, J. Meteor. Soc. Jpn, 89, 283–290, 2011b.

Li, Y. and Thompson, D. W. J.: The signature of the stratospheric Brewer–Dobson circulation in tropospheric clouds, J. Geophys. Res., 118, 3486–3494, doi:10.1002/jgrd.50339, 2013.

Madden, R. A. and Julian, P. R.: Observations of the 40–50-day tropical oscillation – a review, Mon. Weather Rev., 122, 814–837, 1994.

Plumb, R. A. and Eluszkiewicz, J.: The Brewer–Dobson circulation: dynamics of the tropical upwelling, J. Atmos. Sci., 56, 868–890, 1999.

Randel, W. J., Garcia, R. R., and Wu, F.: Time-dependent upwelling in the tropical lower stratosphere estimated from the zonal-mean momentum budget, J. Atmos. Sci., 59, 2141–2152, 2002.

Taguchi, M.: Latitudinal extension of cooling and upwelling signals associated with stratospheric sudden warmings, J. Meteorol. Soc. Jap., 89, 571–580, 2011.

Thuburn, J. and Craig, G. C.: Stratospheric influence on tropopause height: the radiative constraint, J. Atmos. Sci., 57, 17–28, 2000.

Ueyama, R., Gerber, E. P., Wallace, J. M., and Frierson, D. M. W.: The role of high-latitude waves in the intraseasonal to seasonal variability of tropical upwelling in the Brewer–Dobson circulation, J. Atmos. Sci., 70, 1631–1648, 2013.

Winker, D. M., Hunt, W. H., and McGill, M. J.: Initial performance assessment of CALIOP, Geophys. Res. Lett., 34, L19803, doi:10.1029/2007GL030135, 2007.

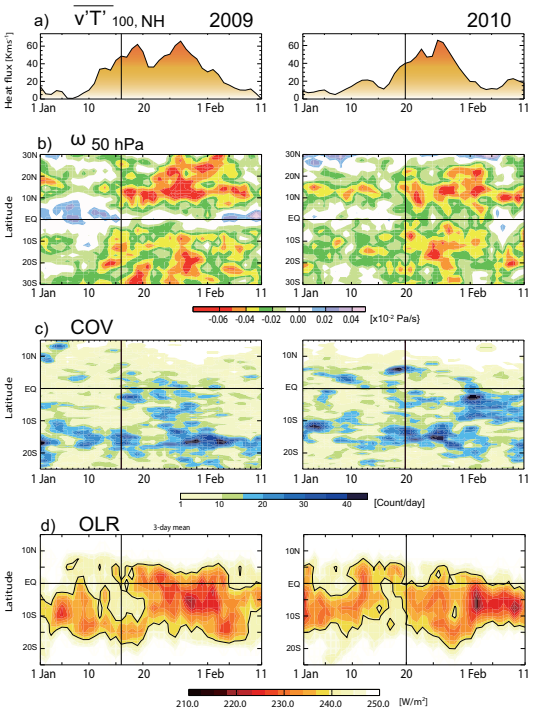

Figure 1. (a) Time series of the eddy heat flux at 100 hPa averaged over 45° N–75° N (K ms^{-1}). **(b)** Zonal mean pressure coordinate vertical velocity at 50 hPa (Pa s^{-1}). **(c)** Number of convective overshootings per day at each latitude. **(d)** Zonal mean OLR (W m^{-2}). Variables are displayed from 1 January to 11 February. Left- and right-hand panels are for 2009 and 2010, respectively. Vertical velocity and OLR data are smoothed by a three-day running mean.

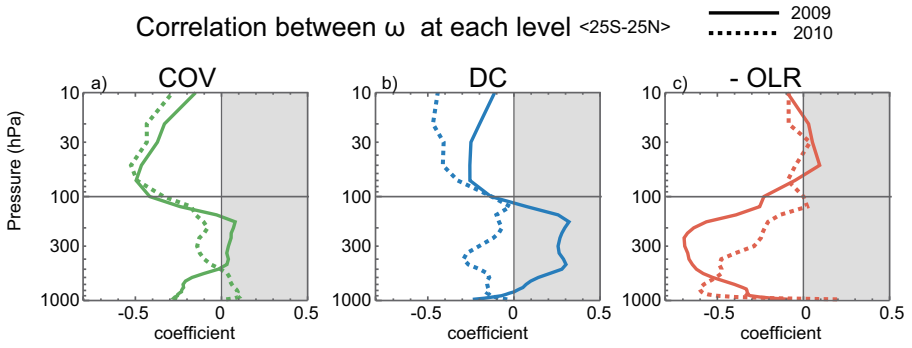

Figure 2. (a) Correlation coefficient between the pressure coordinate vertical velocity (ω) at each pressure level and the daily convective overshooting occurrence frequency (COV) averaged over the tropics. **(b)** As for **(a)**, but for deep convection (DC). **(c)** As for **(a)**, but for the correlation coefficient with –OLR. Variables were first averaged over 25° S to 25° N and then the correlation was calculated over 31 days centered at the onset day (16 January in 2009 and 20 January in 2010). Solid and dashed lines indicate 2009 and 2010, respectively.

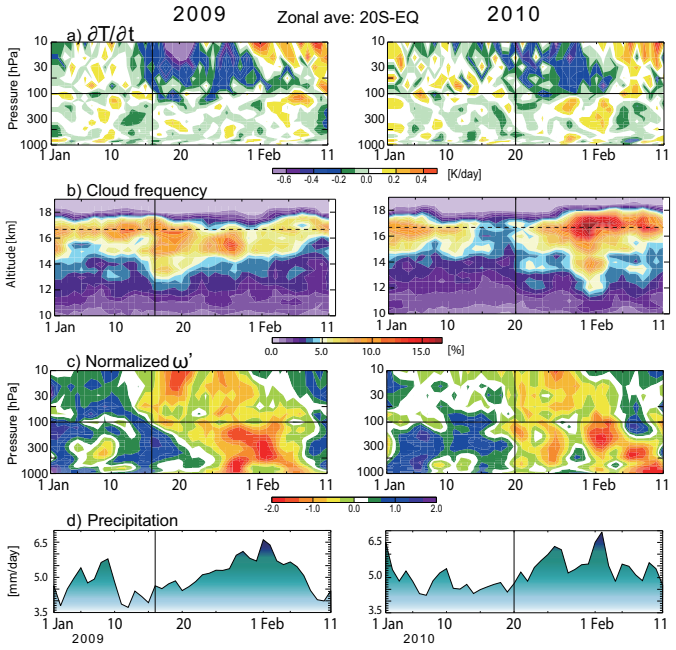

Figure 3. (a) Similar to Fig. 1, except for the pressure–time section of the zonal mean temperature tendency averaged over the SH tropics (20° S to the equator) (K day^{-1}). **(b)** As for **(a)**, except for the geographical altitude–time section of cloud frequency measured by CALIOP (%). **(c)** As for **(a)**, except for the pressure coordinate vertical velocity anomalies normalized by the standard deviation of daily variability. **(c)** Time series of the daily TRMM surface precipitation averaged over SH tropics (mm day^{-1}). Horizontal solid lines in **(a)** and **(c)** and dashed lines in **(b)** indicate 100 hPa pressure level.

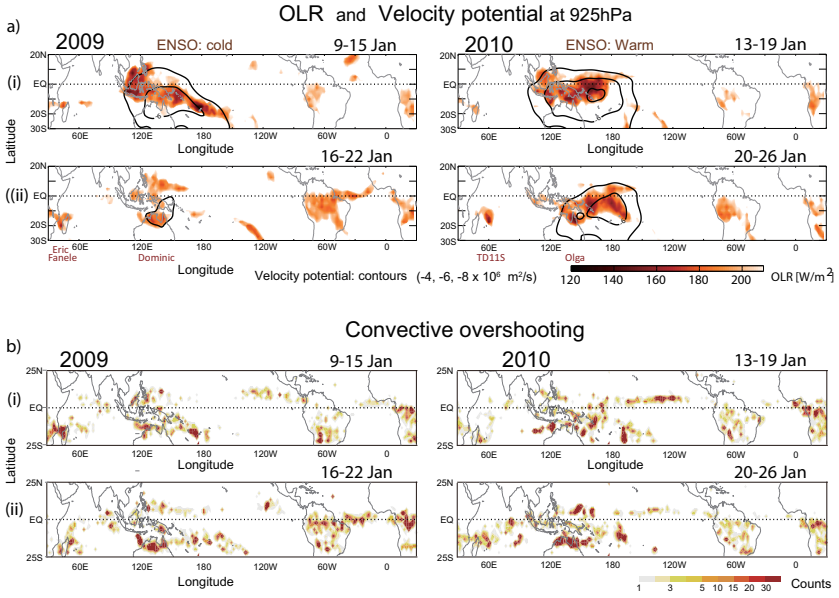

Figure 4. (a) Seven-day mean OLR before (i), and after (ii) the onset of the event. The velocity potential at 925 hPa is also displayed in contours of −4, −6, and -8×10^6 m^2 s^{-1}. **(b)** As for **(a)**, except for the occurrence number of COV during seven days in each 2.5° lat/lon grid box. Left- and right-hand panels are for January 2009 and January 2010, respectively. Labels below panels in **(a)** indicate the names of tropical cyclones and storms.

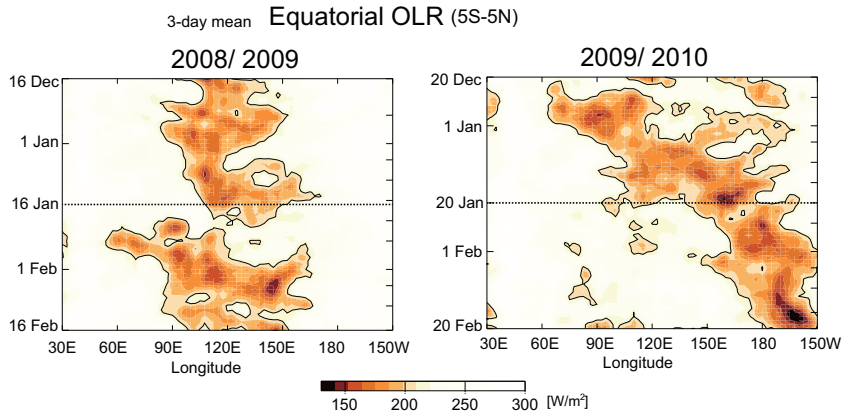

Figure 5. Time–longitude sections of three-day running mean equatorial (5° S–5° N) OLR over the Indian Ocean–central Pacific sector (30° E–150° W) during boreal winter for (left) 2008/09 and (right) 2009/10. The figure displays a two-month period centered on the onset day of the tropical stratospheric upwelling events (16 January 2009 and 20 January 2010) indicated by horizontal solid lines.